4. Numerical Analysis of Spherical Helical Antennas

Numerical techniques are often the only way to predict antenna properties. The spherical helix is best investigated with numerical methods to determine radiation properties, because analytical solutions are not available. In this chapter, the effects of size and number of turns on radiation characteristics of the spherical helix are investigated. Furthermore, properties of novel variations of the spherical helix, such as double spherical helix and hemispherical helix, are studied.

Important properties such as gain, radiation pattern, and input impedance are obtained using the ESP code (Electromagnetic Surface Patch). Then, the axial ratio and total gain are calculated using the output data from the ESP analysis. These quantities are not directly provided by the ESP. The special cases where the spherical helix and hemispherical helix provide nearly circularly polarized far fields are given. The numerical results in this chapter will be compared with measurements in Chapter 5.

4.1 Electromagnetic Surface Patch Code

Electromagnetic Surface Patch Code was first developed at the Ohio State University. The code, written in FORTRAN language can be used to analyze antenna properties such as current distribution, input impedance, gain patterns, and radiation

the method of moments.

The compact size of the ESP program (about 300 Kbytes) allows it to be installed

of an input file or through a subroutine called WEGOM. Since the computations in this work involve a variety of spherical helices, defining their
WEGOM is recommended in order to reduce the compiling time. Source codes of the subroutine WEGOM for several
hemispherical, and double spherical helices are given in the Appendix A.

4.2 Calculation of Directivity and Axial Ratio

These quantities should be calculated using the orthogonal q and f components of gain. The details of directivity and axial ratio calculations are explained below.

4.2.1 Directivity

The ESP code computes the antenna radiation efficiency, e, and the two components of the gain, G_q and G_f. The total gain, G, is then obtained as

$$G = G_q + G_f . \qquad (4.1)$$

It is emphasized that G_q and G_f are obtained by the ESP in decibel-isotropic units. Thus, they must be converted to dimensionless values before being used in (4.1). The computed results for the total gain from (4.1) and the radiation efficiency, e, are used to calculate the directive gain, D_G

$$D_G = \frac{G}{e}. \tag{4.2}$$

Directive gains in all directions are computed and compared to find the maximum value. This maximum is the directivity of the antenna.

4.2.2 Axial Ratio

The axial ratio is a quantitative measure of the state of polarization of an antenna. It is defined as the ratio of the major axis to the minor axis of the polarization ellipse [19]. If the axial ratio is unity the antenna is circularly polarized, while if it is infinity the antenna is linearly polarized. If the axial ratio is somewhere in between, the polarization is elliptical. The axial ratio is expressed as

$$AR = \frac{\left|\vec{E}_{\max}\right|}{\left|\vec{E}_{\min}\right|} = \frac{\left(\sqrt{\left|E_q\right|^2 + \left|E_f\right|^2}\right)_{\max}}{\left(\sqrt{\left|E_q\right|^2 + \left|E_f\right|^2}\right)_{\min}}. \tag{4.3}$$

The ratio of the q and f components of the gain is related to the ratio of the corresponding radiation intensities and field components as

$$\frac{G_q}{G_f} = \frac{U_q}{U_f} = \frac{E_q{}^2}{E_f{}^2}, \tag{4.4}$$

where U denotes the radiation intensity.

If the phase difference between the E_q and E_f components of the electric field is s, the axial ratio is calculated from [20].

$$\mathrm{AR} = \frac{\sqrt{\left[\left|E_q\right|^2 + \left|E_f\right|^2 + \sqrt{\left|E_q\right|^4 + \left|E_f\right|^4 + 2\left|E_q\right|^2\left|E_f\right|^2 \cos(2s)}\right]}}{\sqrt{\left[\left|E_q\right|^2 + \left|E_f\right|^2 - \sqrt{\left|E_q\right|^4 + \left|E_f\right|^4 + 2\left|E_q\right|^2\left|E_f\right|^2 \cos(2s)}\right]}}. \tag{4.5}$$

Then, from (4.4) and (4.5), it is concluded that

$$\mathrm{AR} = \frac{\sqrt{\left[G_q + G_f + \sqrt{G_q{}^2 + G_f{}^2 + 2G_q G_f \cos(2s)} \right]}}{\sqrt{\left[G_q + G_f - \sqrt{G_q{}^2 + G_f{}^2 + 2G_q G_f \cos(2s)} \right]}}. \qquad (4\text{-}6)$$

4.3 Numerical Analysis of Spherical Helices

This section investigates radiation properties of spherical helices calculated from the ESP code. The main purpose is to examine variations of gain, radiation pattern, and axial ratio versus the helix geometry (number of turns and circumference). Both full and truncated geometries are considered. Arrays of two spherical or truncated spherical helices are also discussed.

4.3.1 Spherical and Truncated Spherical Helices

The numerical results presented in this subsection are for spherical helices of 0.01846 meter in radius and mounted over a solid square ground plane of 0.1 meter on each side. A wire diameter of 0.002 meter is considered in the simulations. An earlier investigation by Cardoso [2] revealed that a 10-turn full spherical helix provides circular polarization when $C = 1.25l$ ($f = 3.232$ GHz). So, we focus attention on examining the spherical and truncated spherical helices with $N = 10$. The effects of the actual number of turns (n) on radiation properties are studied. The study is later expanded to the truncated spherical helices with $N = 7$ and $N = 4$. It is emphasized that n represents the actual number of turns, while N is the number of turns if the sphere is fully wound.

4.3.1.1 Truncated Spherical Helices with $N = 10$

Figure 4.1 illustrates radiation patterns in the $y = 0$ plane for 3,5,7, and 9-turn truncated spherical helices when $N = 10$ computed using ESP. It is noted that all patterns exhibit a common property of broad beamwidth, but the magnitudes of q and f components differ significantly with the number of turns. This implies that while the shape of the radiation pattern is not much sensitive to the actual number of turns, the polarization may be affected dramatically. The effect on polarization is more clearly demonstrated in Figures 4.2 and 4.3, which show the phase difference between the q and f components of the electric field and the axial ratio, respectively. As noted in Figure 4.2, only for the 9-turn helix the phase difference is close to 90°. Figure 4.3 reaffirms this fact, as the axial ratio is less than 3 dB when the number of turns is between 9 to 10.

The directivity of a truncated spherical helix exhibits a rather peculiar behavior with the number of turns. The directivity may be examined in two regions, as shown in Figure 4.4. In region I, where $1 < n \le 6$, the directivity is about 9 dB and higher than that of a full spherical helix. In region II, where $6 < n \le 10$, the directivity is lower than that of region I by about 2 dB.

4.3.1.2 Truncated Spherical Helices with $N = 4$ and $N = 7$

Variations of radiation properties with the number of turns when $N = 4$ and 7; that is, when fully wound sphere has 4 or 7 turns, have also been examined. The circumference, C, and the frequency remain the same as those for the case $N = 10$. Figures 4.5 and 4.6 show simulation results for the axial ratio in the $q = 0^\circ$ direction and the directivity, respectively. Generally, fluctuations of the axial ratio versus the actual number of turns are less. In fact, it appears that for smaller N, the axial ratio varies more smoothly with n. As Figure 4.6 indicates, variations of the directivity versus the number of turn are small, implying that the number of turns does not strongly affect the directivity. This is in contrast to the conventional helix in which the directivity increases

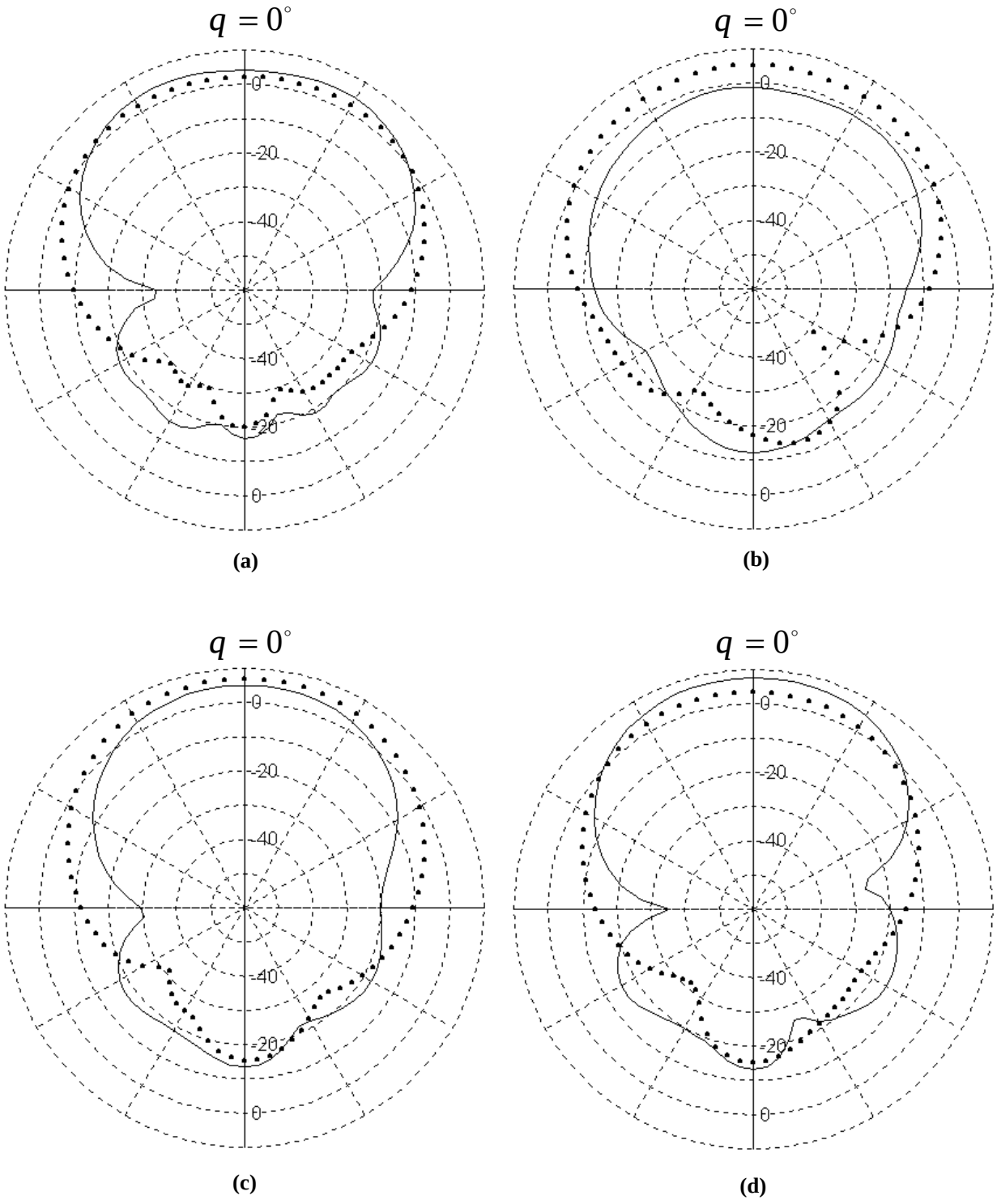

Figure 4.1 **Computed radiation patterns, (———) G_q and (·····) G_f, for truncated spherical helices with $C = 1.25\,l$, $N = 10$, and actual number of turns (a) $n = 9$, (b) $n = 7$, (c) $n = 5$, and (d) $n = 3$.**

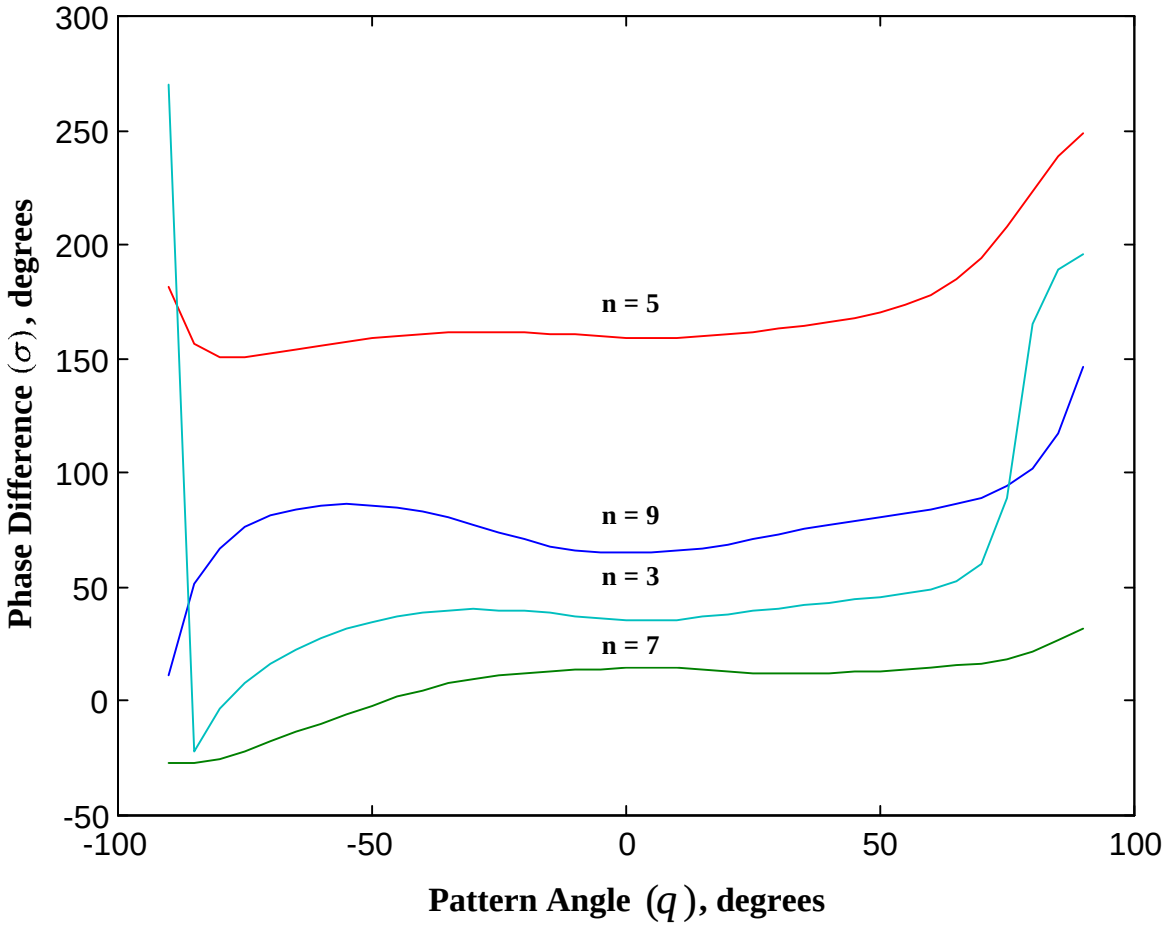

Figure 4.2 **Variations of phase difference between q and f components of electric field versus theta for several values of n**

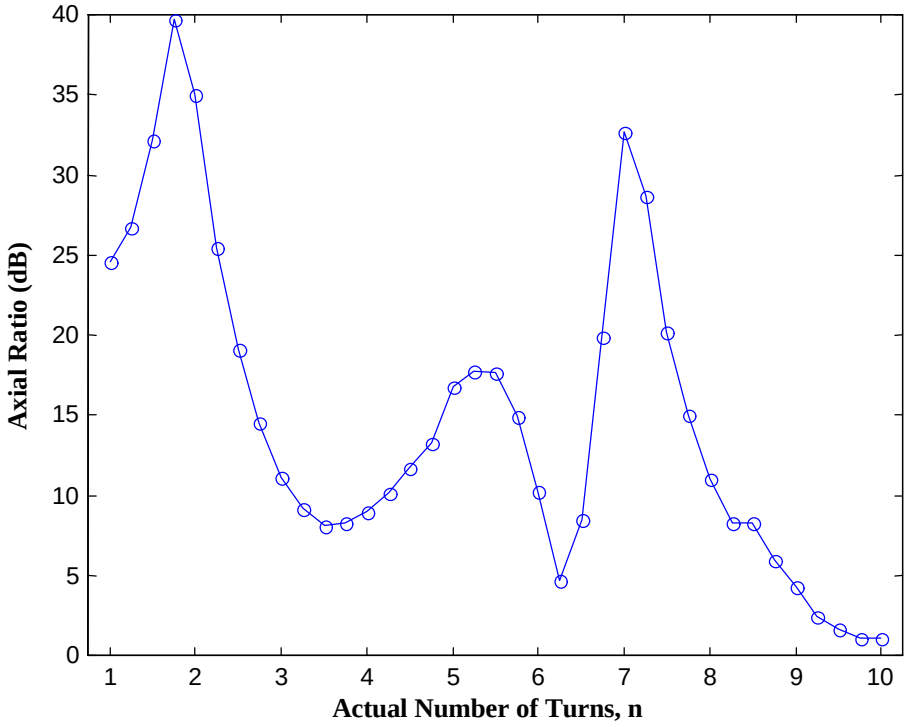

Figure 4.3 **Variations of axial ratio in the $q = 0^{\circ}$ direction versus actual number of turns for truncated spherical helices with $= 1.25l$ and $N = 10$.**

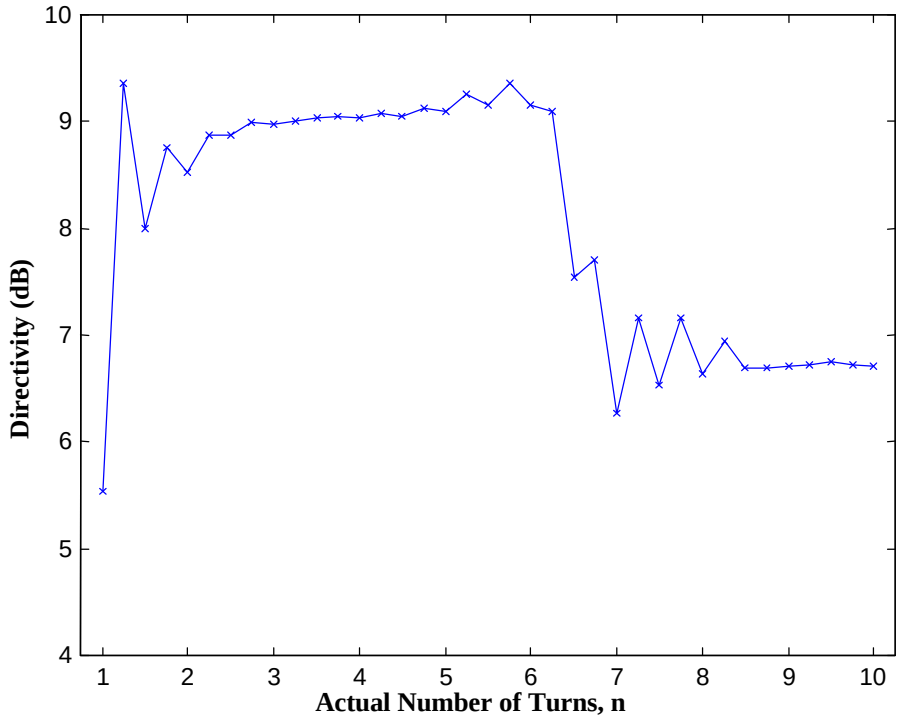

Figure 4.4 **Variations of directivity versus actual number of turns for truncated spherical helices with $C = 1.25l$ and $N = 10$.**

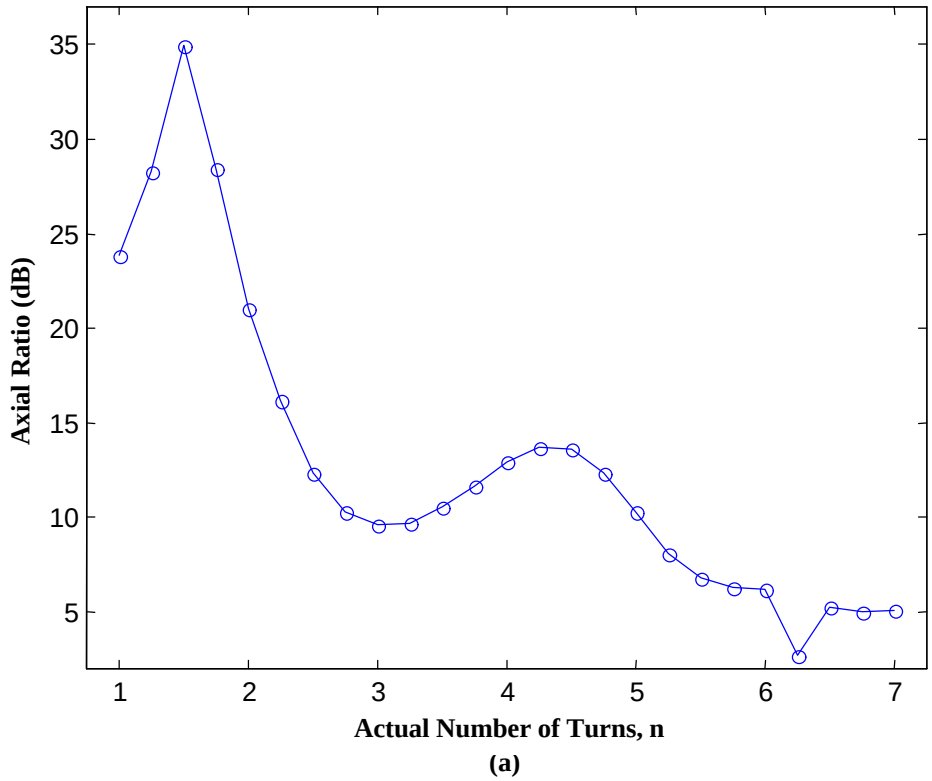

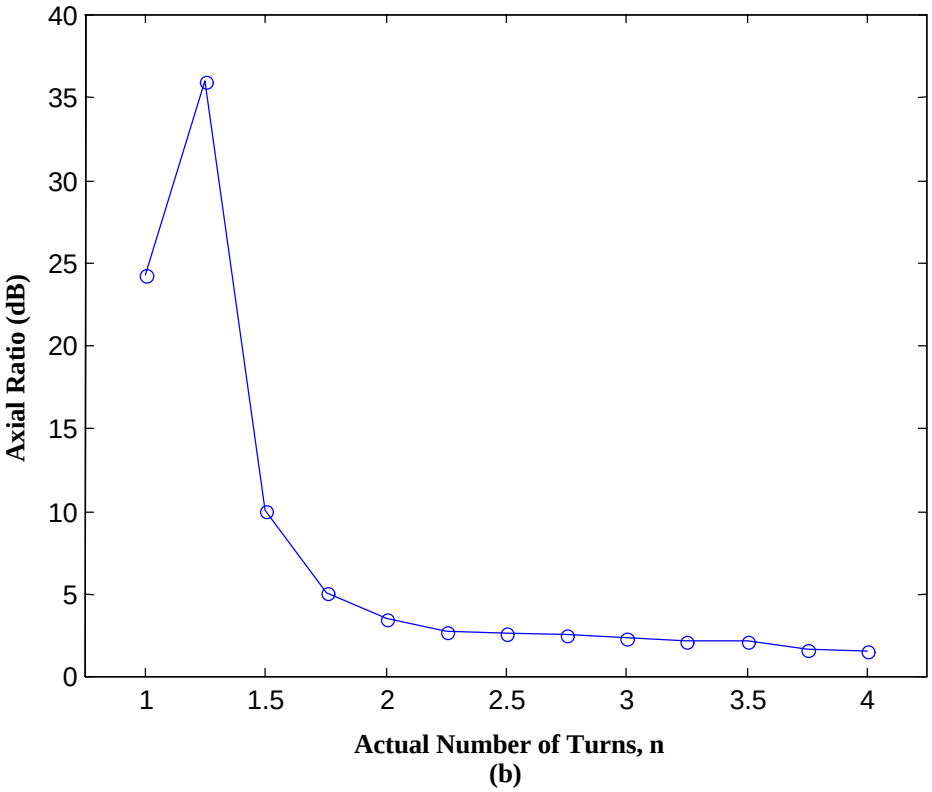

Figure 4.5 **Variations of axial ratio in the $q = 0^\circ$ direction versus actual number of turns for spherical helices with $C = 1.25l$ and (a) $N = 7$, (b) $N = 4$.**

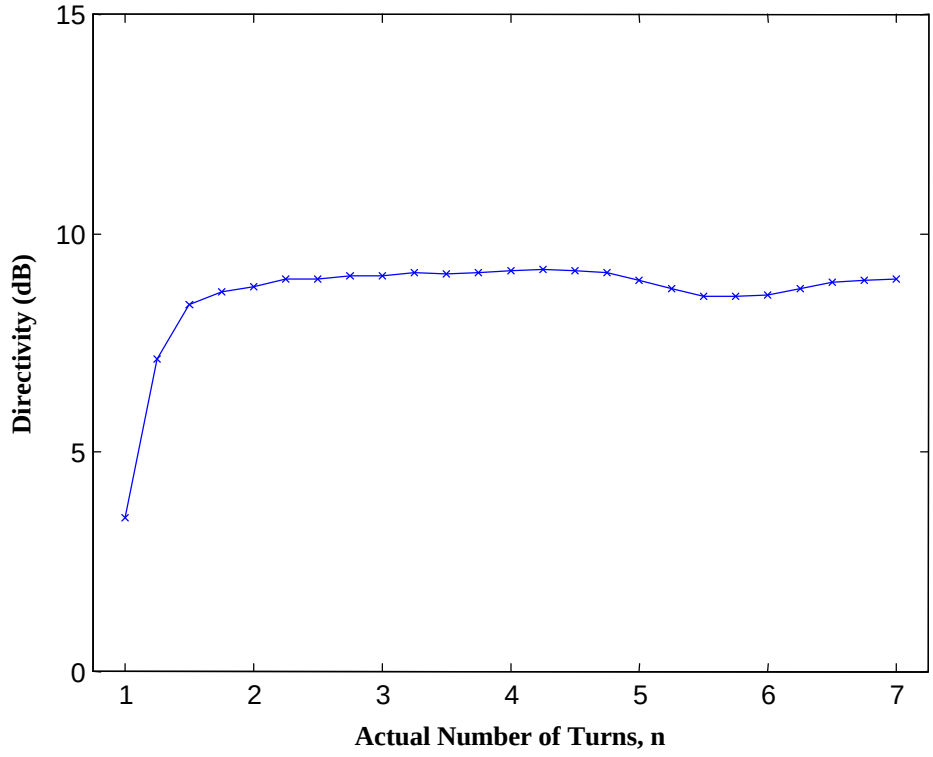

(a)

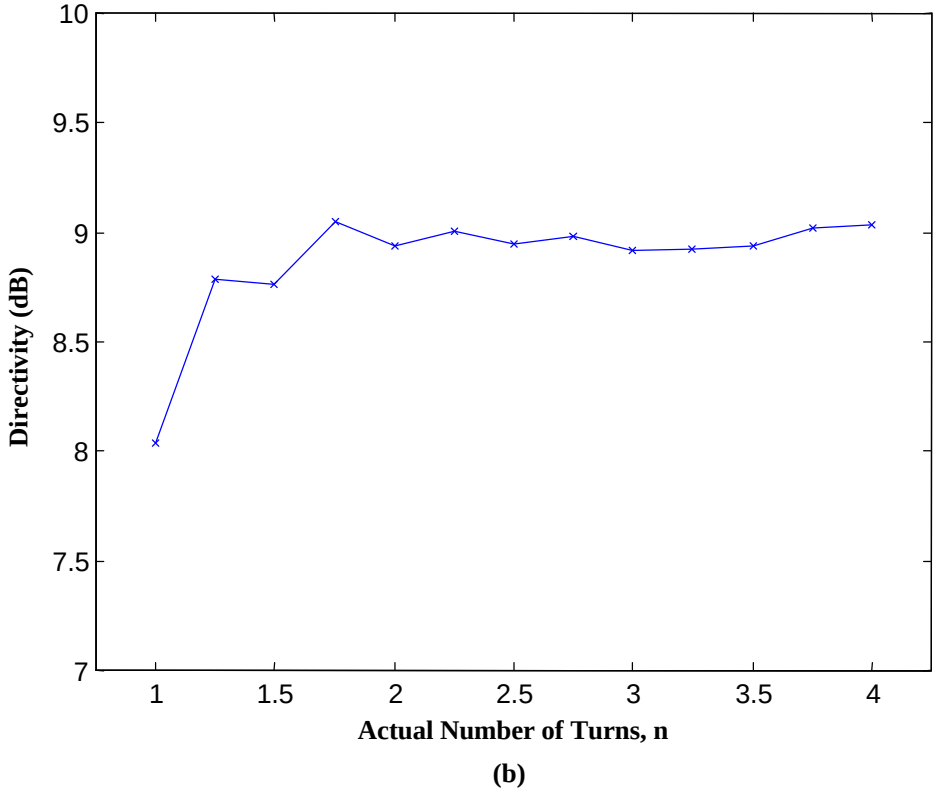

(b)

Figure 4.6 **Variations of directivity versus actual number of turns for spherical helices with** $C = 1.25\,l$ **and (a)** $N = 7$**, (b)** $N = 4$**.**

significantly with number of turns. This behavior may in fact be used to reduce the size of the antenna while maintaining about the same directivity. A hemispherical helix is a special case that will be discussed in Section 4.5.

4.3.2 Double Spherical Helix

From the results in Section 4.3.1, it is apparent that adding more turns does not significantly improve the gain of a spherical helix. A possible approach to increasing the gain would be to form an array of spherical helices. To gain some insight, a simple case referred to as the double spherical helix is studied. Figure 4.7 shows the geometry of the double spherical helix.

Many different cases of the double spherical helix were studied. The results for a representative case are given here. The double spherical helix studied consists of a full 7-turn spherical helix at the base followed by a truncated spherical helix with 4 turns. Both spheres have the same radius of 0.0254 meter. A vertical piece of wire with a length of 0.005 meter is added to the base of the first sphere before it is attached to the ground plain. This piece of wire is to allow room for securing the antenna above the ground plane as is explained in Chapter 5; see Section 5.1 on fabrication of prototype spherical helices. This short piece is included in the simulation analyses so that a more realistic comparison of numerical and measured results can be made. Figure 4.8 compares the directivity of double spherical helix with that of a spherical helix. An improvement of about 2.0 dB in directivity is noted. This increase is attributed to narrowing of the main beam as seen in Figure 4.9, which shows the radiation pattern of the double spherical helix. Figure 4.10 illustrates the axial ratio of the double spherical helix at $f = 1.88$ GHz. It is observed that nearly circular polarization can be achieved over the main beam. The axial ratio is less than 3 dB for $|q| < 25^\circ$. However, circular polarization is only maintained over a narrow bandwidth. Variations of axial ratios versus frequency for several angles are depicted in Figure 4.11. It is noted that only in the frequency range 1.85 GHz < f < 1.88 GHz, AR is less than 3 dB. This corresponds to a bandwidth of

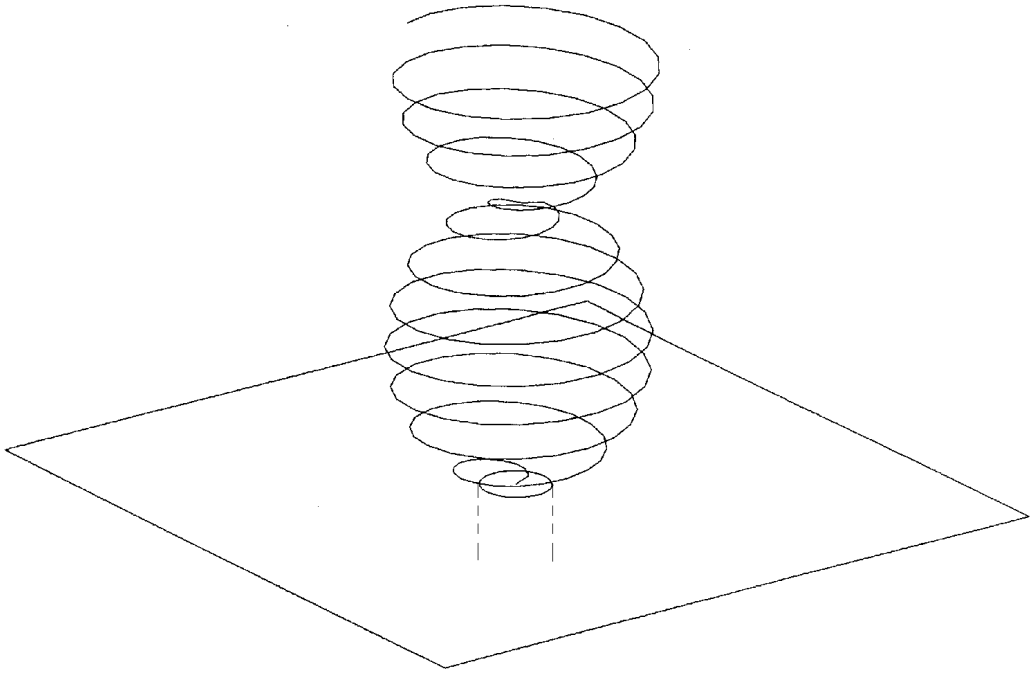

Figure 4.7 **Geometry of double spherical helix. The lower sphere has 7 turns, while the upper one has 4 turns**

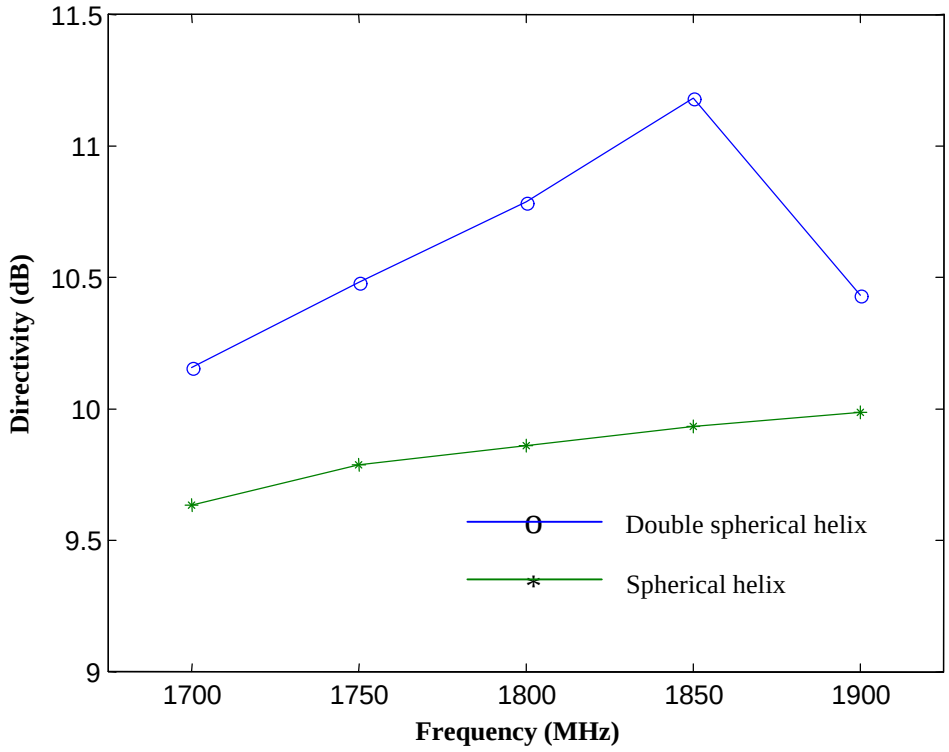

Figure 4.8 **Comparison of computed directivities of the spherical and double spherical helices. Both helices have a radius of 0.0254 m.**

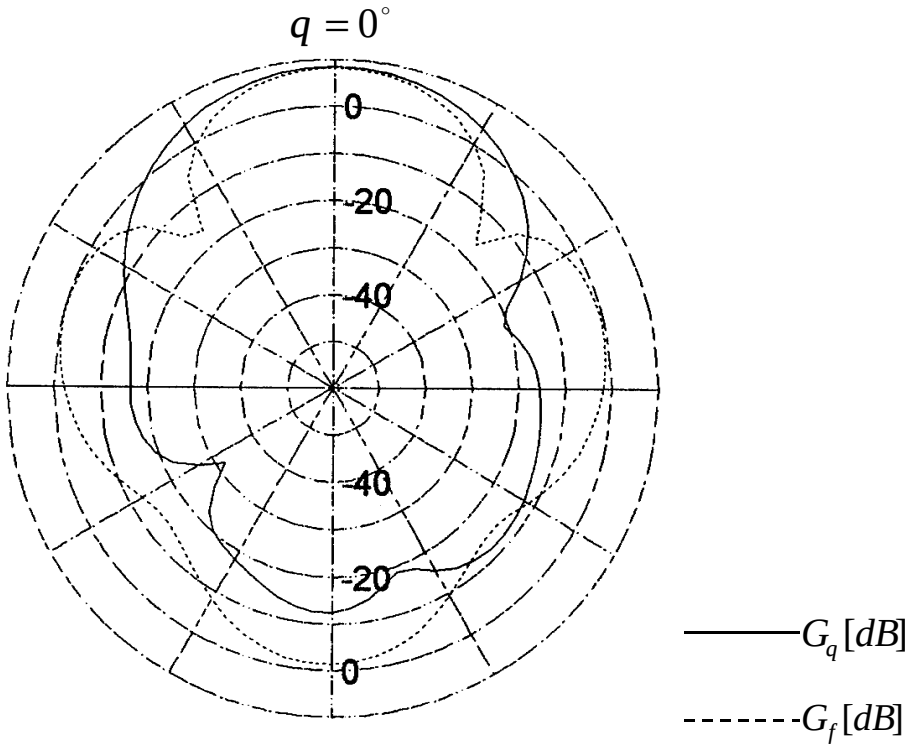

Figure 4.9 **Calculated radiation patterns of double spherical helix at** $f = 1.88$ **GHz**

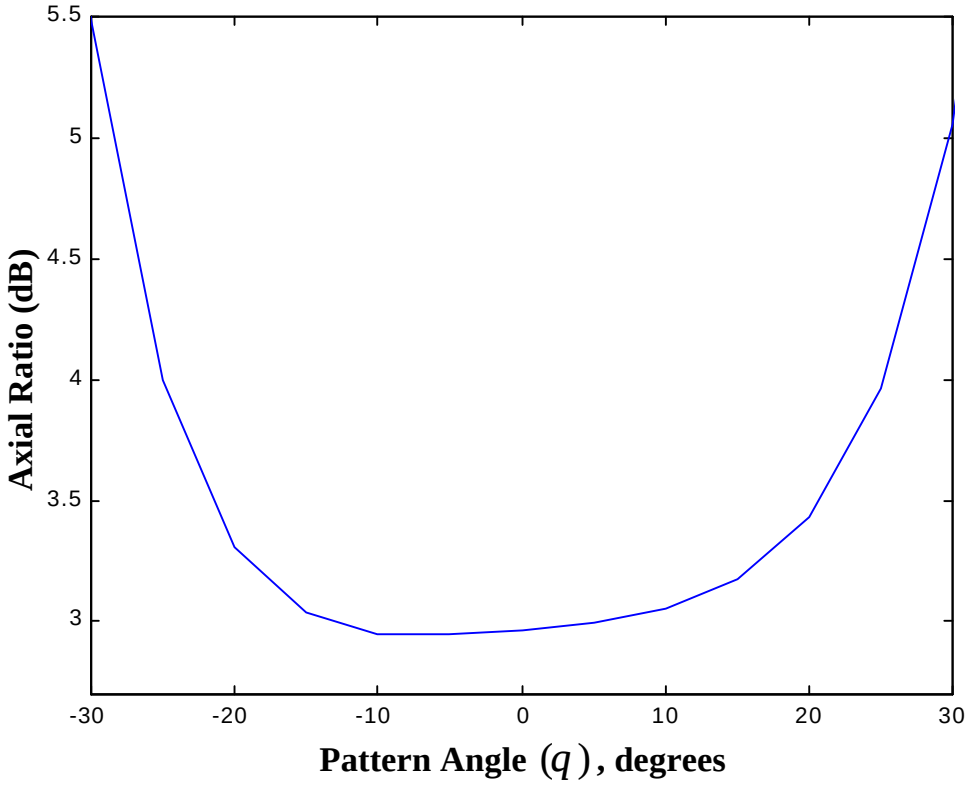

Figure 4.10 **Axial ratio of double spherical helix at** $f = 1.88$ **GHz**

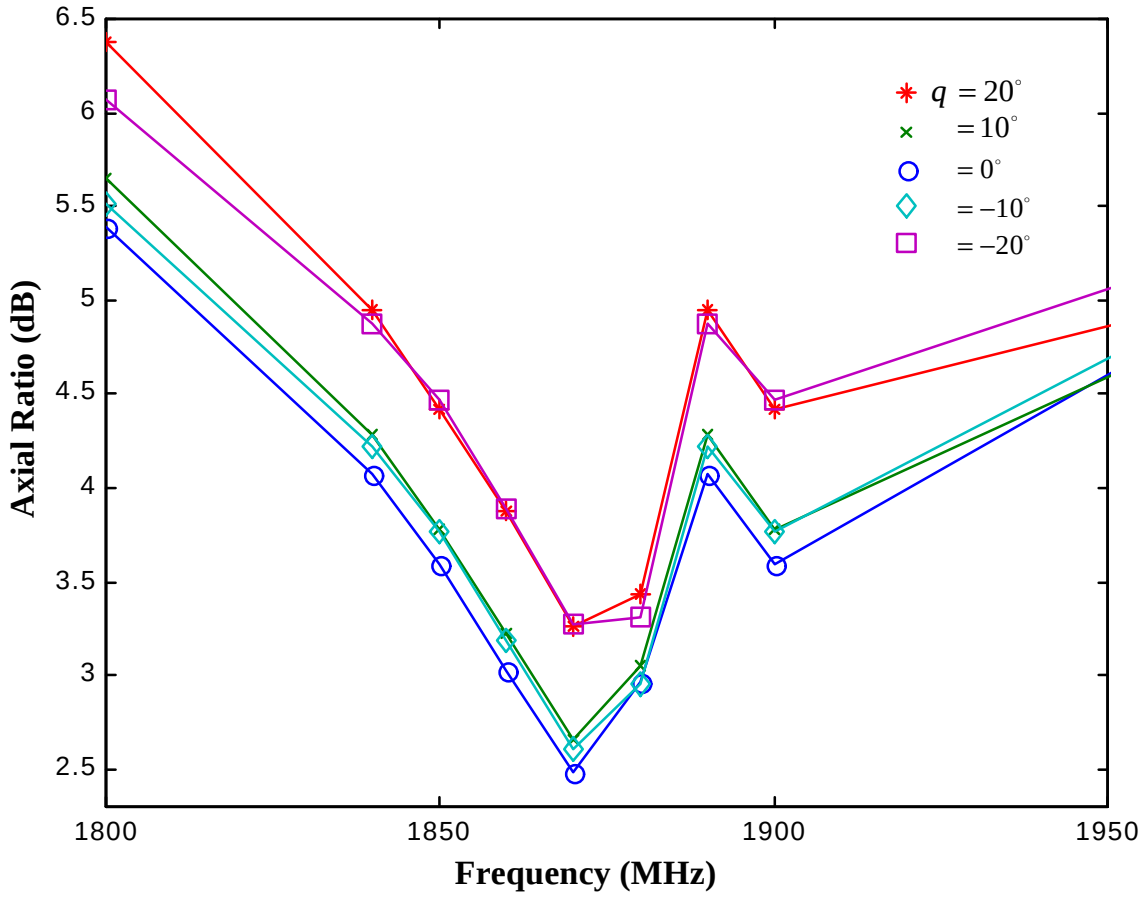

Figure 4.11 **Calculated axial ratio versus frequency for double spherical helix with a diameter of** 0.0508 m.

about 30 MHz. Thus, the application of circularly polarized double spherical helix is limited to situations where narrow bandwidths are required.

4.4 Hemispherical Helix

The idea of a hemispherical helix is based on the fact that most of the radiation properties of the spherical helix (far-field patterns, directivity, half-power beamwidth, but not polarization) do not significantly change with the actual number of turns. This antenna, when properly designed, should behave nearly the same as the corresponding full spherical helix but with half the volume. This section examines the radiation properties of hemispherical helices a wide range of frequencies. Comparison of radiation properties of hemispherical helices with different number of turns reveals that a 4.5-turn hemispherical helix provides an overall better performance. The geometry of a 4.5-turn hemispherical helix is shown in Figure 3.2. As in the case of the double spherical helix, a short piece of wire with a length of 0.005 meter is added to the base of the antenna in order to avoid a short circuit with the ground plane.

4.4.1 Optimum Design

In order to determine the number of turns such that the hemispherical helix provides a nearly optimum performance, variations of directivity, axial ratio, and input impedance versus the number of turns were examined. The number of turns was varied between 3 and 10 in increments of 0.5 turns. In order to explain the process for determining the number of turns for an optimum, the results for 3, 4.5, 7, and 9 turns are presented. Figures 4.12 and 4.13 compare the directivity and the axial ratio, respectively, for hemispherical helices with the actual number of turns equal to 3, 4.5, 7, and 9. All four hemispherical helices have the same size and a circumference of 1.19λ at the mid-band frequency. It is noted from Fig. 4.12 that directivities is not strongly affected by the

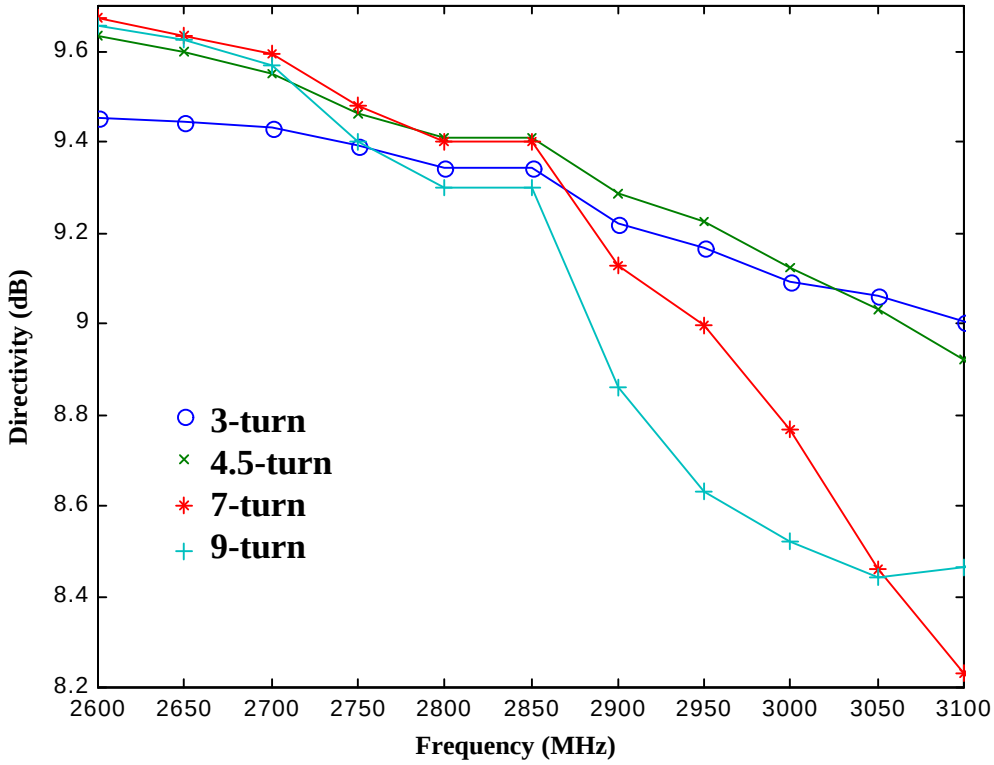

Figure 4.12 **Comparison of directivity versus frequency for various hemispherical helices.**

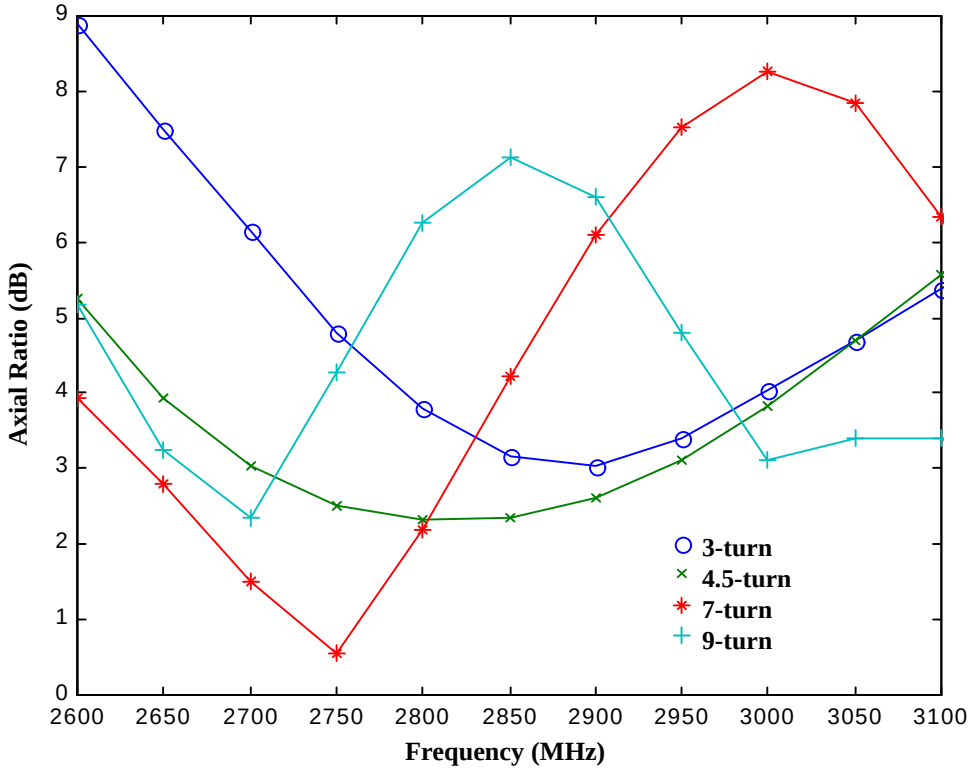

Figure 4.13 **Comparison of axial ratio in $q = 0^\circ$ direction versus frequency for various hemispherical helices**

number of turns, particularly in the lower frequency range. However, as Fig. 4.13 indicates, the axial ratio is influenced more strongly by the number of turns. The 3-turn hemispherical helix exhibits an axial ratio of larger than 3 dB over the entire frequency range, and thus is not a good candidate as a circularly polarized antenna. The hemispherical helices with 4.5, 7, and 9 turns are all capable of providing less than 3 dB axial ratio each over a certain frequency range. However, the axial-ratio bandwidth is smaller for larger number of turns. In other words, the bandwidth for the 4.5 turn antennas is wider than the bandwidth of those with 7 and 9 turns. Next, the input impedance is examined. Figures 4.14 to 4.17 illustrate the real and imaginary parts of the input impedance for 3-, 4.5-, 7-, and 9-turn hemispherical helices, respectively. The radiation resistance of the 3-turn antenna fluctuates considerably with frequency. The other three antennas have fairly flat radiation resistance curves, but variations in the imaginary parts are larger for the antenna with a larger number of turns. This should be expected, because a hemispherical helix with a large number of turns behaves more as a cavity than a radiator. Overall, the 4.5-turn antenna provides a better performance with regard to the axial ratio and input impedance. A more in-depth investigation of the 4.5-turn hemispherical helix is presented below.

4.4.2 Radiation Properties

Now attention is focused on the radiation properties of the 4.5-turn hemispherical helix. The directivity and the input impedance of this antenna were already addressed in the previous section. In summary, the directivity of the 4.5-turn hemispherical helix, as seen in Fig. 4.12, is about 9 dB over the frequency range 2700 MHz < f < 3000 MHz. The real part of the input impedance is between 120-150 ohms, while the imaginary part varies from –50 ohms to +40 ohms in the above frequency range; see Fig. 4.15. The far-field patterns at a frequency of 2.84 GHz ($C = 1.19\lambda$) are shown in Figure 4.18. At this frequency the minimum boresight ($q = 0$) axial ratio occurs. Radiation patterns of this antenna at several other frequencies in the range 2650 MHz < f < 3050 MHz ($1.11\lambda < C < 1.26\lambda$) are presented in the Appendix C. A common feature of the patterns

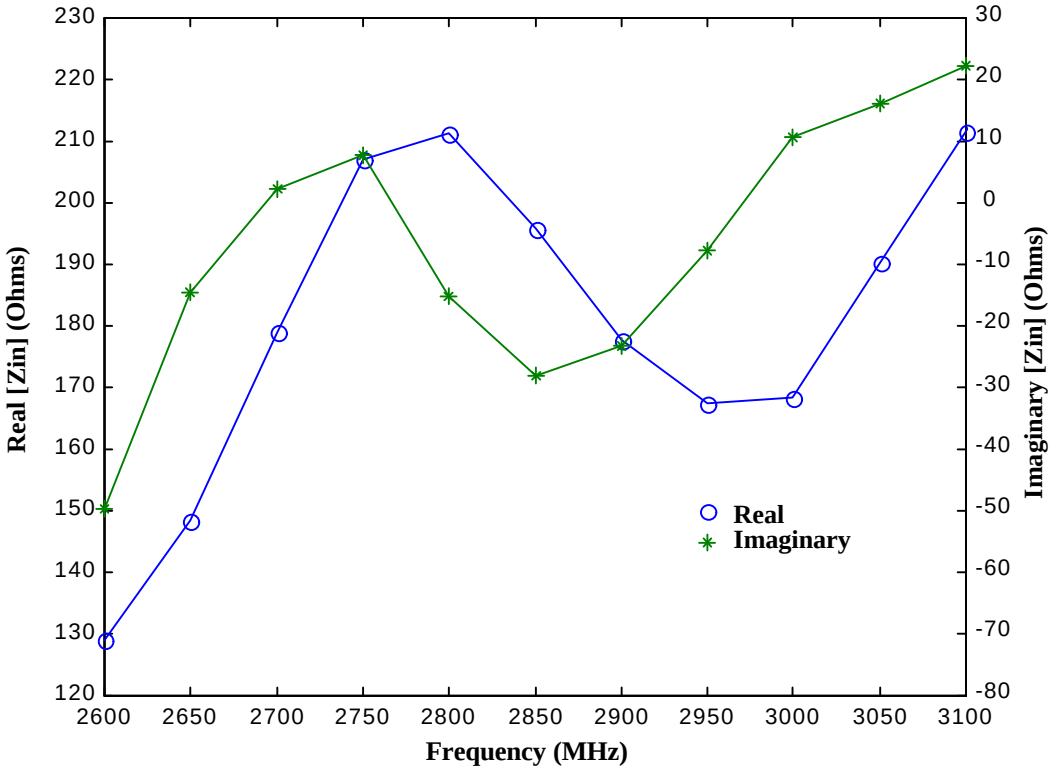

Figure 4.14 **Input impedance versus frequency for 3-turn hemispherical helix with a diameter of 0.04 m.**

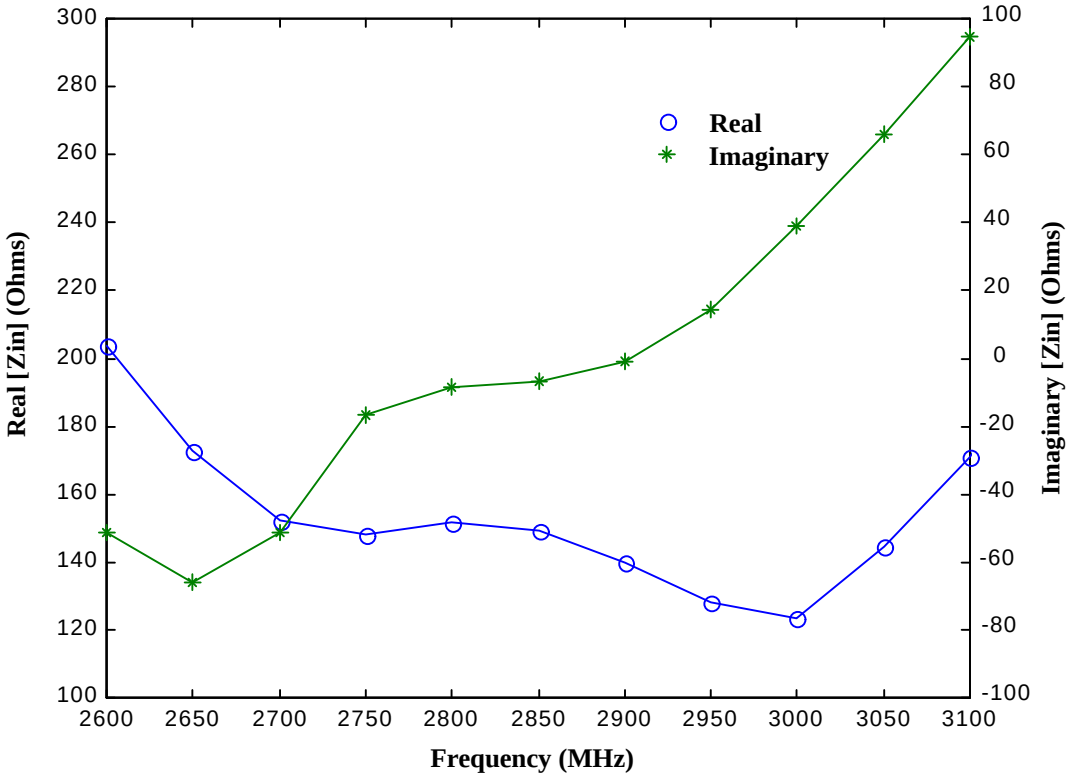

Figure 4.15 **Input impedance versus frequency for 4.5-turn hemispherical helix with a diameter of 0.04 m.**

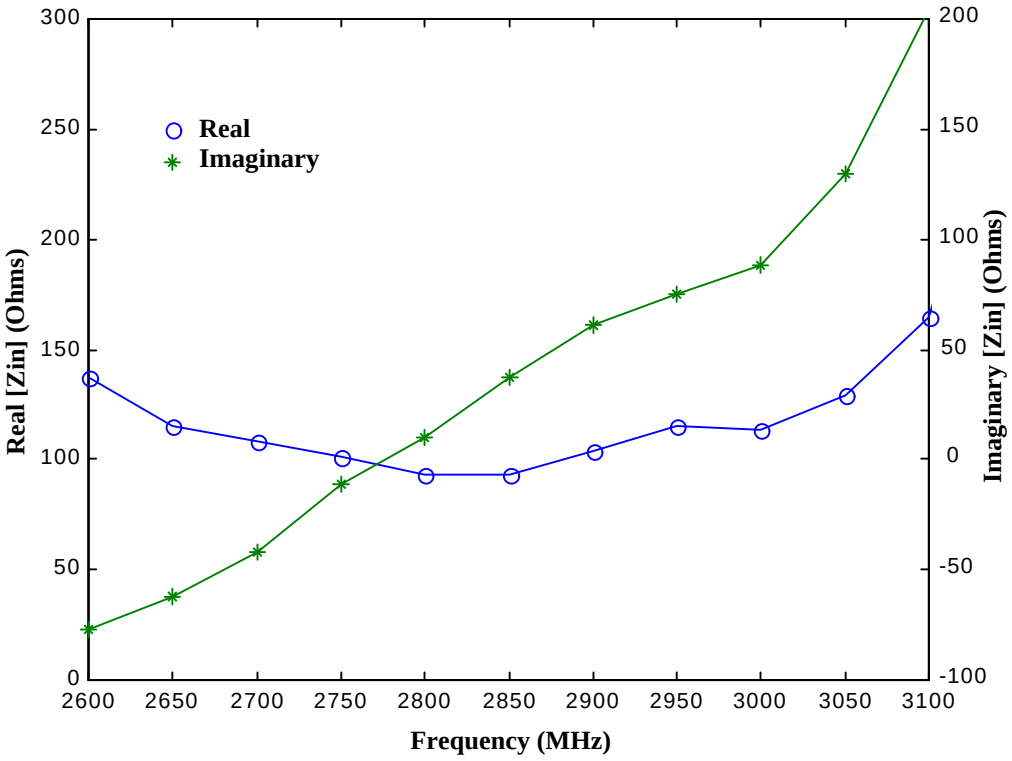

Figure 4.16 **Input impedance versus frequency for 7-turn hemispherical helix with a diameter of 0.04 m.**

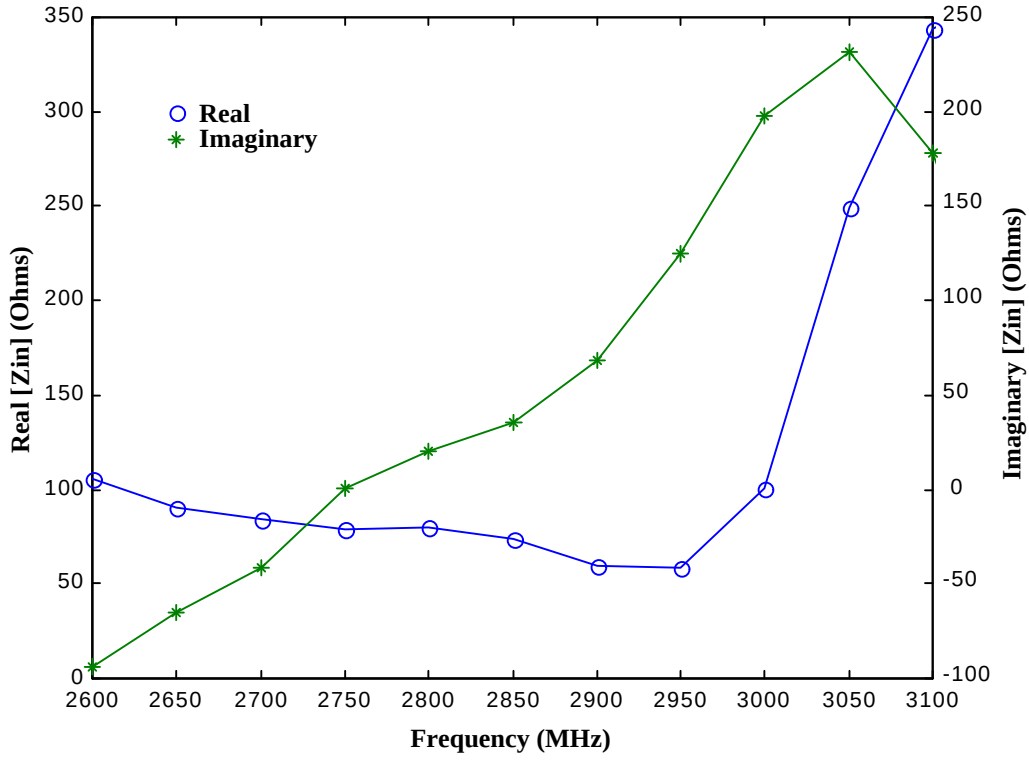

Figure 4.17 **Input impedance versus frequency for 9-turn hemispherical helix with a diameter of 0.04 m.**

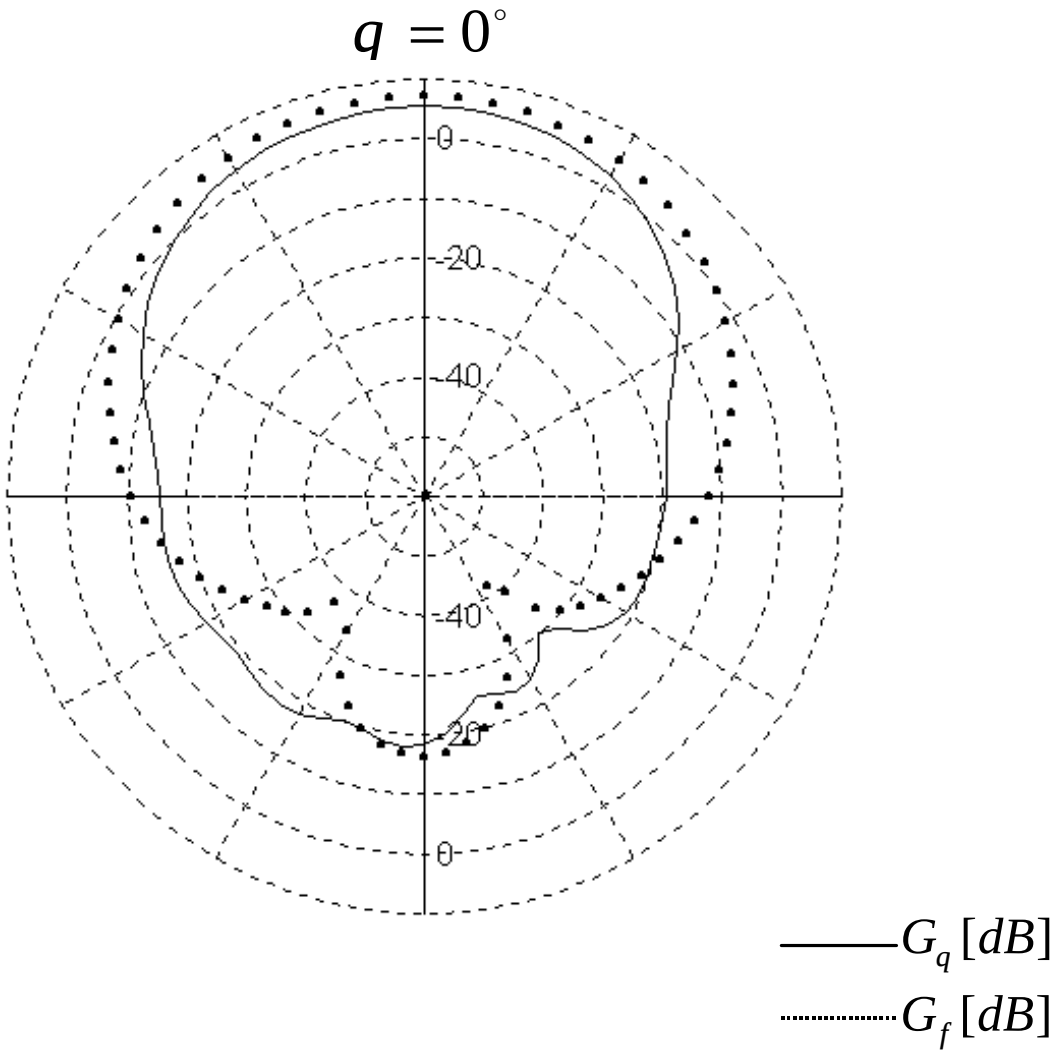

Figure 4.18 **Computed far-field patterns at $f = 2.84$ GHz for a 4.5-turn hemispherical helix with a diameter of 0.04 m. mounted over 10x10 cm^2 ground plane.**

is that all have a broad main beam with a half-power beamwidth of about 80 degrees and no distinct side lobes. The front-to-back ratio is better than 25 dB in all patterns.

Figure 4.19 illustrates variations of the axial ratio versus frequency for the 4.5-turn hemispherical helix. It is noted that the axial ratio remains below 3 dB (for $q = 0$) over the frequency range 2700 MHz < f < 2950 MHz; that is, over a bandwidth of 250 MHz. The 3-dB axial ratio bandwidth for other values of θ is narrower. Thus, the bandwidth of this antenna may be estimated to be around 200 MHz. Variations of the axial ratio versus θ at several other frequencies in the above frequency range for the 4.5-turn hemispherical helix are presented in the Appendix C.

4.4.3 Frequency Scaling

Based on the principle of frequency scaling, radiation properties of two antennas with the same normalized dimensions (relative to wavelength) are the same. Then, it is possible to resize any antenna by varying its physical dimension for operation at another frequency. That is, if geometrical dimensions of the antenna are changed by a factor of n (including dimensions of ground plain and diameter of wire), the operating frequency has to be changed by a factor of $1/n$ in order to have the same radiation characteristics. To verify if the ESP code abide by this principle, we examine the radiation characteristics of several, physically different but electrically the same, 4.5-turn hemispherical helices. Figures 4.20 and 4.21 compare the radiation patterns and the axial ratios of four 4.5-turn hemispherical helices at the frequencies 2.84 GHz, 5 GHz, 7 GHz, and 9 GHz. All four antennas have identical electrical dimensions. It is noted that the radiation patterns are essentially the same, but measurable differences among the axial ratios exist. These differences may be attributed to different computation (round off, truncation, etc.) errors at different frequencies, primarily in the phases of field components. Despite the small variations in the axial ratio, this test indicates a hemispherical helix designed for operation at a certain frequency can be scaled in dimensions for operation at another frequency.

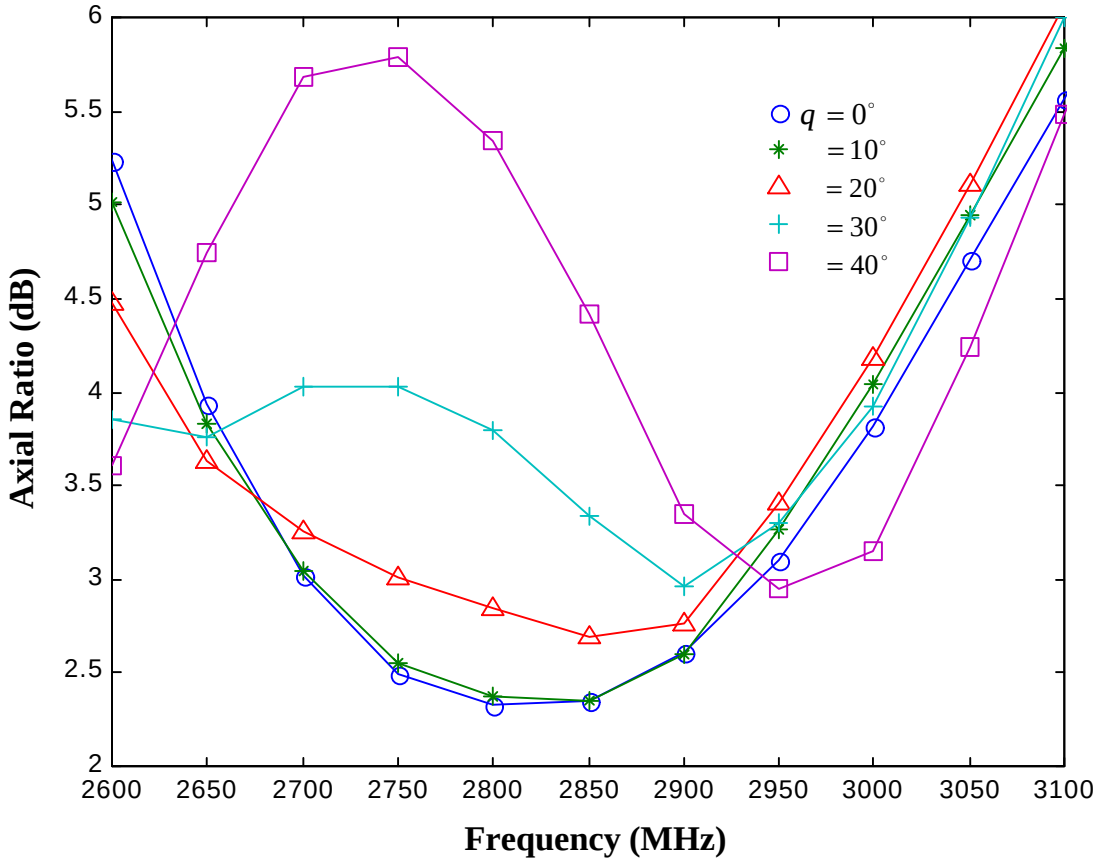

Figure 4.19 **Axial ratio versus frequency for 4.5-turn hemispherical helix with a diameter of 0.04 m.**

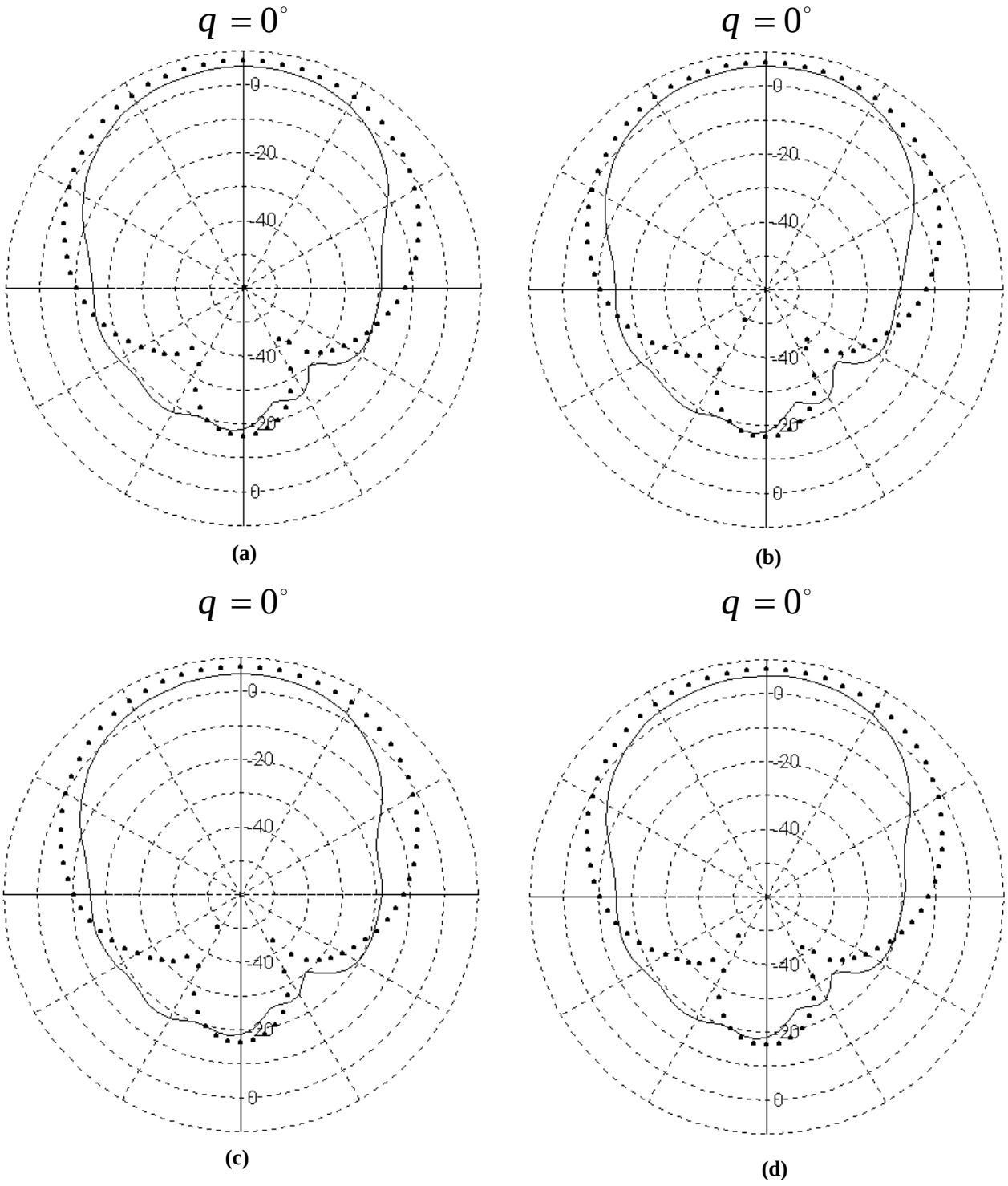

Figure 4.20 **Computed radiation patterns, (_____) G_q and (.....) G_f, for 4.5-turn hemispherical helices with normalized circumference of $1.19\,l$, (a) $f = 2.84$ GHz, (b) $f = 5.0$ GHz, (c) $f = 7.0$ GHz, and (d) $f = 9.0$ GHz.**

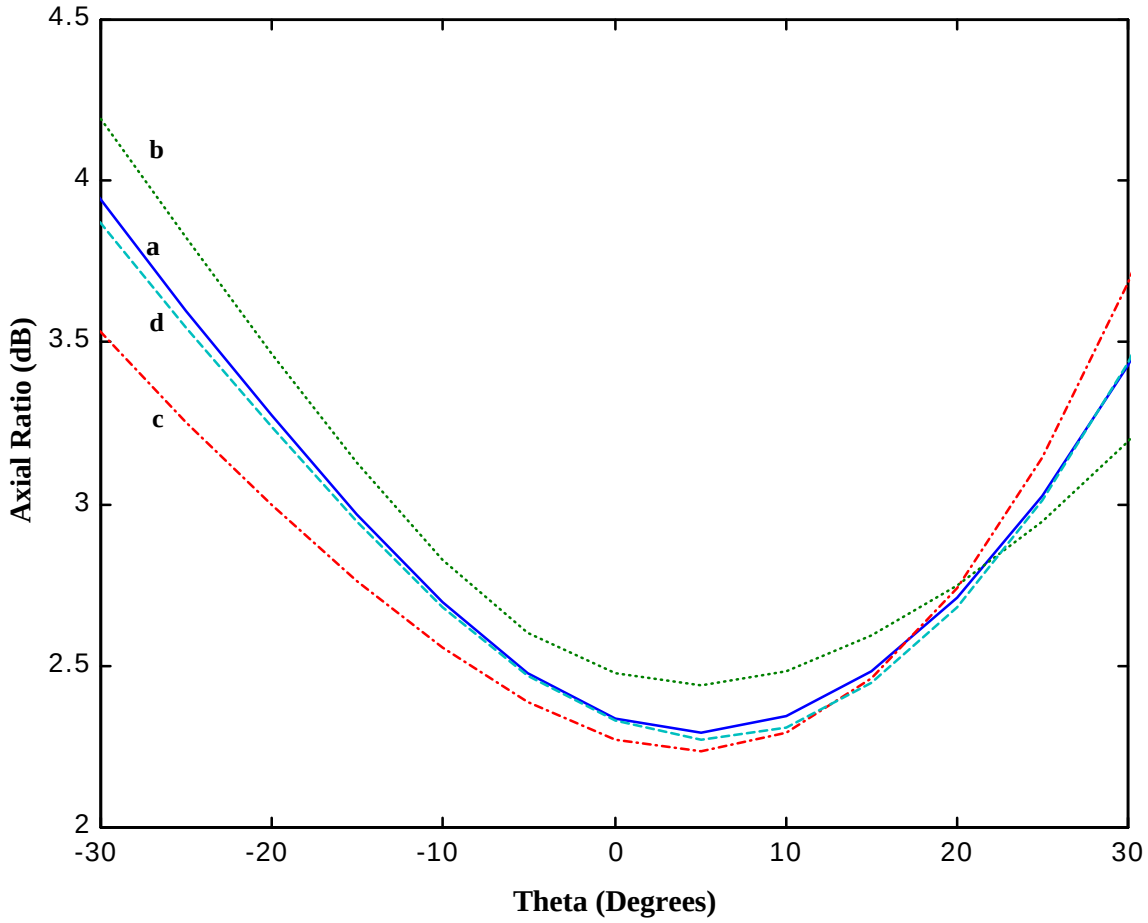

Figure 4.21 **Axial ratios for 4.5-turn hemispherical helices with normalized circumference of** $1.19\,l$ **, (a)** $f = 2.84$ **GHz, (b)** $f = 5.0$ **GHz, (c)** $f = 7.0$ **GHz, and (d)** $f = 9.0$ **GHz.**